

## The Preparation and Crystal Structure of $(\beta)6\text{SbF}_3 \cdot 5\text{SbF}_5$ †

W. A. Shantha Nandana, Jack Passmore,\* and Peter S. White\*

Department of Chemistry, University of New Brunswick, Fredericton, New Brunswick, Canada E3B 6E2

$(\beta)6\text{SbF}_3 \cdot 5\text{SbF}_5$  was prepared by the reduction of  $\text{SbF}_3 \cdot \text{SbF}_5$  with a slight excess of phosphorus trifluoride relative to the stoichiometric amount, in arsenic trifluoride solution. It was also prepared by the reduction of antimony pentafluoride in sulphur dioxide solution and a stoichiometric quantity of iodine. The Raman spectrum of  $(\beta)6\text{SbF}_3 \cdot 5\text{SbF}_5$  is identical to that of a material designated  $\text{SbF}_3 \cdot \text{SbF}_5$  (**B**) by previous workers. A single-crystal *X*-ray diffraction study of  $(\beta)6\text{SbF}_3 \cdot 5\text{SbF}_5$  shows that it is monoclinic, space group  $P2_1/c$  with cell dimensions  $a = 11.638(1)$ ,  $b = 8.995(1)$ ,  $c = 16.723(2)$  Å,  $\beta = 106.81(1)^\circ$ , and  $Z = 2$ . The structure was refined to a final  $R$  of 0.041 for 2 440 reflections. The structure consists of discrete  $\text{Sb}_6\text{F}_{13}^{5+}$  cations and  $\text{SbF}_6^-$  anions with cation–anion interactions. The cation can be viewed as being built of strongly interacting  $\text{Sb}_2\text{F}_5^+$  and  $\text{SbF}_2^+$  units. The geometries of the fluorine atoms about the various  $\text{Sb}^{\text{III}}$  species are described and discussed. The structure of  $(\beta)6\text{SbF}_3 \cdot 5\text{SbF}_5$  is similar to, but different from,  $(\alpha)6\text{SbF}_3 \cdot 5\text{SbF}_5$ , previously prepared at high temperatures by the fluorination of antimony metal.

Two adducts having very different Raman spectra were both assigned the composition  $\text{SbF}_3 \cdot \text{SbF}_5$  by Gillespie and co-workers<sup>1</sup> on the basis of elemental analyses. One adduct, designated  $\text{SbF}_3 \cdot \text{SbF}_5$  (**A**), was prepared from an excess of antimony pentafluoride and antimony trifluoride, and the other labelled  $\text{SbF}_3 \cdot \text{SbF}_5$  (**B**), was prepared from an excess of antimony pentafluoride and elemental antimony, both reactions using sulphur dioxide as solvent. The adduct  $\text{SbF}_3 \cdot \text{SbF}_5$  (**A**) was subsequently prepared by the reaction of an excess of antimony pentafluoride and  $\text{S}_4\text{N}_4$ , and the 1:1 stoichiometry  $\text{SbF}_3 \cdot \text{SbF}_5$  established from an *X*-ray structure determination.<sup>2</sup> Raman spectra of single crystals of  $\text{SbF}_3 \cdot \text{SbF}_5$  and bulk  $\text{SbF}_3 \cdot \text{SbF}_5$  (**A**) were shown to be identical.

Edwards and Slim<sup>3</sup> prepared  $6\text{SbF}_3 \cdot 5\text{SbF}_5$  by the direct fluorination of elemental antimony and determined its *X*-ray crystal structure. Later Holloway and co-workers<sup>4</sup> prepared the same material in a similar reaction, and characterised it as such from the cell parameters obtained from single crystals. Single-crystal Raman spectra were similar to those of  $\text{SbF}_3 \cdot \text{SbF}_5$  (**B**) and it was inferred that  $\text{SbF}_3 \cdot \text{SbF}_5$  (**B**) was in fact the compound  $6\text{SbF}_3 \cdot 5\text{SbF}_5$  described by Edwards and Slim.<sup>3</sup> In the course of a systematic study of the reduction of  $\text{SbF}_3 \cdot \text{SbF}_5$  (**A**) we obtained single crystals whose Raman spectra were identical to that of  $\text{SbF}_3 \cdot \text{SbF}_5$  (**B**) and very similar to, but definitely different from, that reported by Holloway and co-workers<sup>4</sup> for  $6\text{SbF}_3 \cdot 5\text{SbF}_5$ . We therefore determined the *X*-ray crystal structure of our product and show that it also has the stoichiometry  $6\text{SbF}_3 \cdot 5\text{SbF}_5$ , hereafter designated  $(\beta)6\text{SbF}_3 \cdot 5\text{SbF}_5$ , with a different, but similar structure to  $6\text{SbF}_3 \cdot 5\text{SbF}_5$ ,<sup>3</sup> hereafter designated  $(\alpha)6\text{SbF}_3 \cdot 5\text{SbF}_5$ . Various preparations of  $(\beta)6\text{SbF}_3 \cdot 5\text{SbF}_5$  and its *X*-ray crystal structure are reported below.

$(\beta)6\text{SbF}_3 \cdot 5\text{SbF}_5$  is one of a class of binary antimony fluorides that can be regarded as ionic salts of antimony trifluoride and antimony pentafluoride containing the  $\text{SbF}_6^-$  anions and complex  $\text{Sb}^{\text{III}}$  fluorocations linked by fluorine cation–anion interactions. The structures of  $3\text{SbF}_3 \cdot \text{SbF}_5$ ,<sup>5</sup>  $5\text{SbF}_3 \cdot 3\text{SbF}_5$ ,<sup>6</sup>

$2\text{SbF}_3 \cdot \text{SbF}_5$ ,<sup>3,7</sup>  $(\alpha)6\text{SbF}_3 \cdot 5\text{SbF}_5$ ,<sup>3</sup>  $(\beta)6\text{SbF}_3 \cdot 5\text{SbF}_5$ ,  $\text{SbF}_3 \cdot \text{SbF}_5$ ,<sup>2</sup> and  $3\text{SbF}_3 \cdot 4\text{SbF}_5$ <sup>8</sup> have now been determined.

### Experimental

*Reagents and Apparatus.*—Apparatus, chemicals, and techniques, unless otherwise specified, are described in refs. 5 and 9. Elemental antimony was supplied by Anachemia Chemicals Ltd.  $\text{SbF}_3 \cdot \text{SbF}_5$  was prepared according to ref. 10. (However,  $\text{SbF}_3 \cdot \text{SbF}_5$  may contain some impurities.) Weights of reactants and products of the reactions described below, as well as some similar reactions, are given in Table 1. The equations referred to below are those given in Table 1.

*Preparations of  $(\beta)6\text{SbF}_3 \cdot 5\text{SbF}_5$ .*—(a) *By the reaction of  $\text{SbF}_3 \cdot \text{SbF}_5$  and  $\text{PF}_3$  according to equation (1).* A slight excess of phosphorus trifluoride, relative to that calculated by equation (1), was condensed onto a mixture of finely ground  $\text{SbF}_3 \cdot \text{SbF}_5$  over arsenic trifluoride in a well dried Pyrex bulb equipped with a Teflon-stemmed J. Young valve. A translucent crystalline material appeared after standing at room temperature (r.t.) for a day. The reaction was judged complete when practically no  $\text{PF}_3$  was observed in the i.r. spectrum of the gases over the liquid–solid mixture. After 3 d the volatile materials ( $\text{AsF}_3$ ,  $\text{PF}_5$ ; traces of  $\text{OPF}_3$ ,  $\text{PF}_3$ ) were removed leaving a white crystalline product, which was subjected to a dynamic vacuum overnight. The Raman spectra of the single crystals were identical to that of  $\text{SbF}_3 \cdot \text{SbF}_5$  (**B**) and were essentially identical to the Raman spectra of the bulk material. *X*-Ray precession photographs showed the crystals were twinned  $(\beta)6\text{SbF}_3 \cdot 5\text{SbF}_5$ .

(b) *By the reaction of antimony pentafluoride and phosphorus trifluoride according to equation (2).* A slight excess of  $\text{PF}_3$  relative to that calculated according to equation (2) was condensed onto a solution of  $\text{SbF}_5$  in  $\text{AsF}_3$ . A cloudy precipitate appeared ca. 3 h after reaching room temperature, and a translucent highly crystalline product was produced in 2–3 d. Raman spectra and *X*-ray precession photographs of ca. 12 crystals from reaction (2i) indicated the presence of  $(\beta)6\text{SbF}_3 \cdot 5\text{SbF}_5$ ,  $5\text{SbF}_3 \cdot 3\text{SbF}_5$ ,<sup>6</sup> and a material with a cubic unit cell [ $a = 10.1(1)$  Å],<sup>10</sup> possibly  $\text{H}_3\text{O}^+ \cdot \text{SbF}_6^-$ .  $\text{H}_3\text{O}^+ \cdot \text{SbF}_6^-$  can be indexed on a cubic cell of dimensions 10.13 Å,<sup>11</sup> and therefore it is possible that our product is  $\text{H}_3\text{O}^+ \cdot \text{SbF}_6^-$ . Those from reaction (2ii) contained  $(\beta)6\text{SbF}_3 \cdot 5\text{SbF}_5$  and  $5\text{SbF}_3 \cdot 3\text{SbF}_5$ .<sup>6</sup> In both cases *X*-ray photographs revealed that the  $(\beta)6\text{SbF}_3 \cdot 5\text{SbF}_5$  crystals were twinned. The Raman spectra

† Tridecafluoro-hexa-antimony(5+) pentakis[hexafluoroantimonate(1-)].

Supplementary data available (No. SUP 56225, 3 pp.): thermal parameters. See Instructions for Authors, *J. Chem. Soc., Dalton Trans.*, 1985, Issue 1, pp. xvii–xix. Structure factors are available from the editorial office.

**Table 1.** Various preparations of  $(\beta)6\text{SbF}_3 \cdot 5\text{SbF}_5$  and related reactions (weights of compounds in g; values in parentheses in mmol)

$11(\text{SbF}_3 \cdot \text{SbF}_5) + \text{PF}_3 \xrightarrow[\text{r.t.}]{\text{AsF}_3} 2(6\text{SbF}_3 \cdot 5\text{SbF}_5) + \text{PF}_5$ (1)									
$\text{SbF}_3 \cdot \text{SbF}_5 / \text{PF}_3$		$\text{SbF}_3 \cdot \text{SbF}_5$	$\text{PF}_3$	$\text{AsF}_3$	Time (d)	$\text{SbF}_x$	$x^b$		
calc. <sup>a</sup>	obs.								
11.00	10.35	1.884 (4.76)	0.041 (0.46)	16.0	8	1.745	3.25		
$11\text{SbF}_5 + 6\text{PF}_3 \xrightarrow[\text{r.t.}]{\text{AsF}_3} 6\text{SbF}_3 \cdot 5\text{SbF}_5 + 6\text{PF}_5$ (2)									
$\text{SbF}_5 / \text{PF}_3$		$\text{SbF}_5$	$\text{PF}_3$	$\text{AsF}_3$	Time (d)	$\text{SbF}_x$	$x$		
calc. <sup>a</sup>	obs.								
(i)	1.83	4.595 (21.20)	1.092 (12.41)	14.7	13	4.148	3.89		
(ii)	1.83	3.027 (13.97)	0.760 (8.64)	17.3	11	2.705	3.79		
(iii)	1.83	5.820 (26.85)	1.290 (14.66)	$\text{SO}_2^c$ 6.5	14	5.224	3.83		
$35\text{SbF}_5 + 12\text{I}_2 \xrightarrow[\text{r.t.}]{\text{SO}_2} 12\text{I}_2\text{Sb}_2\text{F}_{11} + 6\text{SbF}_3 \cdot 5\text{SbF}_5$ (3)									
$\text{SbF}_5 / \text{I}_2$		$\text{SbF}_5$	$\text{I}_2$	$\text{SO}_2$	Time (d)	$\text{I}_2\text{Sb}_2\text{F}_{11}$		$6\text{SbF}_3 \cdot 5\text{SbF}_5$	
calc. <sup>a</sup>	obs.					calc.	obs.	calc.	obs.
(i)	2.92	6.446 (29.74)	2.500 (9.85)	6.3	5	6.957	7.247	1.769	1.491
(ii)	2.92	3.147 (14.52)	1.173 (4.62)	10.6	9	3.263	3.640	0.829	0.593
(iii)	2.92	6.831 (3.52)	1.006 (4.20)	10.9	5	<i>d</i>			
$6\text{SbF}_5 + 2\text{I}_2 \xrightarrow[\text{r.t.}]{\text{AsF}_3} 2\text{I}_2\text{Sb}_2\text{F}_{11} + \text{SbF}_3 \cdot \text{SbF}_5$ (4)									
$\text{SbF}_5 / \text{I}_2$		$\text{SbF}_5$	$\text{I}_2$	$\text{AsF}_3$	Time (d)	$\text{I}_2\text{Sb}_2\text{F}_{11}$		$\text{SbF}_3 \cdot \text{SbF}_5$	
calc. <sup>a</sup>	obs.					calc.	obs.	calc.	obs.
(i)	3.00	9.769 (45.07)	3.440 (13.55)	11.8	11	9.571	10.430	2.680	2.490
Attempted reaction $12\text{Sb} + 4\text{SbF}_5 \xrightarrow[\text{r.t.}]{\text{SO}_2} 5(6\text{SbF}_3 \cdot 5\text{SbF}_5)$ (5)									
$\text{SbF}_5 / \text{Sb}$		$\text{SbF}_5$	$\text{Sb}$	$\text{SO}_2$	Time (d)	$\text{SbF}_x$			
calc. <sup>a</sup>	obs.								
3.58	6.66	12.577 (58.03)	1.062 (8.72)	8.6	7	<i>e</i>			

<sup>a</sup> Mole ratios calculated according to the corresponding equation. <sup>b</sup> The calculated value of  $x$  for  $6\text{SbF}_3 \cdot 5\text{SbF}_5$  is 3.91. <sup>c</sup> In this reaction,  $\text{SO}_2$  was used as the solvent instead of  $\text{AsF}_3$ . <sup>d</sup> Product weight not recorded but the reduced product was a mixture of microcrystalline  $(\beta)6\text{SbF}_3 \cdot 5\text{SbF}_5$  and crystalline  $\text{SbF}_3 \cdot \text{SbF}_5$ , in approximately 3:2 ratio and identified by Raman spectroscopy. <sup>e</sup> The product weight was not recorded but the Raman spectrum of the white-blue product was similar to that of  $\text{SbF}_3 \cdot \text{SbF}_5$ .

of both bulk materials were consistent with the presence of both  $(\beta)6\text{SbF}_3 \cdot 5\text{SbF}_5$  and  $5\text{SbF}_3 \cdot 3\text{SbF}_5$ .<sup>6</sup> There may also be small amounts of other unidentified products.

Reaction (2) was also carried out using  $\text{SO}_2$  as a solvent, and an exact stoichiometry of  $\text{PF}_3$  and  $\text{SbF}_5$ . On addition of the  $\text{PF}_3$ , a white paste formed, which after ca. 4 h became blue. After another day, a blue solution formed over a whitish solid. The volatile material was removed leaving a bluish-white powder whose Raman spectrum we were unable to obtain.

(e) ~~By the reaction of antimony pentafluoride and iodine according to equation (3).~~ These reactions were carried out in two bulbed vessels, volume ca. 20 cm<sup>3</sup>, connected via a coarse sintered glass frit and equipped with two J. Young valves. One bulb was isolatable from the other by the additional valve. Prewighed amounts of  $\text{SbF}_5$  and  $\text{SO}_2$  were condensed into the

isolatable portion of the vessel. A slight excess of powdered iodine was added to the second bulb through the valve, and this portion of the vessel was subjected to a dynamic vacuum with heating of the Pyrex vessel until the weight of iodine was that reported in Table 1, under equation (3). The  $\text{SbF}_5$ - $\text{SO}_2$  solution was then poured onto the iodine. An immediate deep blue solution with a green tinge was observed. After several days the solution was filtered through the frit and the solvent condensed back onto the insoluble product. On reaching r.t. the solution was again filtered and the process repeated until a colourless insoluble product was obtained (ca. 12 times). The soluble product was a blue-black solid. The magnetic susceptibility of the product,  $\text{I}_2\text{Sb}_2\text{F}_{11}$  [(3i), Table 1], was found to be 2.07 B.M. (lit.,<sup>12</sup> 2.00 B.M.). The insoluble products of reactions (3i) and (3ii) were white highly crystalline solids. Raman spectra of the

**Table 2.** Fractional atomic co-ordinates (with estimated standard deviations in parentheses)

Atom	X/a	Y/b	Z/c	Atom	X/a	Y/b	Z/c
Sb(1)	0.073 29(6)	0.675 96(8)	0.266 05(4)	F(42)	0.055 0(7)	0.198 6(8)	0.003 0(5)
Sb(2)	0.341 98(6)	0.771 90(8)	0.154 22(5)	F(43)	0.142 7(7)	-0.053 9(8)	0.081 2(4)
Sb(3)	-0.158 82(7)	0.521 95(8)	0.034 04(4)	F(51)	-0.109 1(5)	0.679 7(8)	0.290 2(4)
Sb(4)	0.000 00	0.000 00	0.000 00	F(52)	-0.427 6(6)	0.825 0(8)	0.204 4(4)
Sb(5)	-0.271 62(6)	0.751 65(7)	0.250 59(4)	F(53)	-0.264 5(7)	0.703 3(9)	0.143 7(5)
Sb(6)	-0.443 19(7)	0.260 21(8)	0.075 81(4)	F(54)	-0.325 0(8)	0.563 2(9)	0.263 4(6)
F(1)	0.028 5(6)	0.874 3(7)	0.231 5(4)	F(55)	-0.266 8(7)	0.796 7(10)	0.359 8(5)
F(2)	-0.020 4(6)	0.619 9(7)	0.150 3(4)	F(56)	0.206 3(7)	0.436 9(8)	0.257 5(5)
F(3)	0.211 1(6)	0.724 6(7)	0.207 7(4)	F(61)	0.443 1(7)	0.759 3(8)	0.035 4(5)
F(4)	0.409 0(6)	0.586 0(7)	0.186 6(4)	F(62)	-0.569 5(7)	0.393 2(9)	0.044 2(5)
F(5)	-0.224 1(6)	0.358 7(8)	-0.057 0(4)	F(63)	-0.331 1(6)	0.419 0(8)	0.082 6(4)
F(6)	0.102 7(6)	0.853 1(7)	0.399 5(4)	F(64)	0.431 2(7)	0.794 8(9)	0.309 9(4)
F(7)	0.000 0	0.500 0	0.000 0	F(65)	-0.309 0(6)	0.138 5(9)	0.108 9(5)
F(41)	-0.073 5(7)	0.042 2(8)	0.083 1(4)	F(66)	-0.545 0(8)	0.101 7(10)	0.070 7(6)

bulk product and individual crystals were identical to one another and to that reported for  $\text{SbF}_3 \cdot \text{SbF}_5$  (**B**) [( $\beta$ ) $6\text{SbF}_3 \cdot 5\text{SbF}_5$ , see Table 3]. Single crystals from preparation (3ii) were used for the X-ray crystal structure determination. A similar reaction, but with liquid  $\text{AsF}_3$  as solvent leads to  $\text{SbF}_3 \cdot \text{SbF}_5$ ,<sup>9</sup> [reaction (4), Table 1].

(d) *Reaction of an excess of  $\text{SbF}_5$  with elemental antimony in sulphur dioxide solution.* An excess of  $\text{SbF}_5$  was reacted with powdered antimony metal in a Pyrex vessel equipped with a J. Young Teflon-in-glass valve. A light blue solution over a white solid was given after 1 d. The volatiles were removed yielding a white solid with a bluish tinge with a Raman spectrum corresponding to that of  $\text{SbF}_3 \cdot \text{SbF}_5$ .<sup>1</sup> [Data are presented under reaction (5), Table 1.]

*Crystal Data.*— $6\text{SbF}_3 \cdot 5\text{SbF}_5$ ,  $M = 2156.2$ , monoclinic, space group  $P2_1/c$ ,  $a = 11.638(1)$ ,  $b = 8.995(1)$ ,  $c = 16.723(2)$  Å,  $\beta = 106.81(1)^\circ$ ,  $U = 1675.8(4)$  Å<sup>3</sup>,  $Z = 2$ ,  $D_c = 4.70$  Mg m<sup>-3</sup>,  $F(000) = 1896$ ,  $\lambda = 0.71069$  Å,  $2\theta_{\text{max}} = 50^\circ$ ; 2946 unique reflections, 2440 observed reflections [ $I \geq 2\sigma(I)$ ], crystal size  $0.20 \times 0.20 \times 0.24$  mm.

A suitable crystal was sealed in a glass capillary tube under an atmosphere of dry  $\text{N}_2$ . The crystal was initially aligned on a precession camera after which it was transferred to a Picker FACS-I diffractometer equipped with graphite-monochromated Mo- $K_\alpha$  radiation. Cell parameters and an orientation matrix were determined by a least-squares fit to the centred coordinates of 12 Friedel pairs of reflections in the range  $30 \leq 2\theta \leq 50^\circ$ . Intensity data were collected using  $\omega$ - $2\theta$  scans at  $2^\circ (2\theta) \text{ min}^{-1}$ . Background intensity was estimated by a standing count of one-tenth of the scan time at each end of the scan; if the reflection was considered significant [ $I > 2\sigma(I)$ ] an analysis of the peak profile was performed.

The structure was solved using the MULTAN-80 system<sup>13</sup> of direct methods programs. After correction of the data for absorption the structure was refined by block-matrix least-squares techniques using weights derived from counter statistics. Scattering factors were taken from ref. 14 and corrected for anomalous dispersion; the function minimised was  $\Sigma w(\Delta|F|)^2$ . All atoms were assigned anisotropic thermal parameters. The final residuals were  $R = (\Sigma \Delta|F|/\Sigma|F|) = 0.041$  and  $R' = [w(\Delta|F|)^2/\Sigma w|F|^2] = 0.061$  (including unobserved reflections, 0.053 and 0.067 respectively). Atomic co-ordinates are given in Table 2. The programs used were those of Larson and Gabe<sup>15</sup> for the PDP8/A computer.

## Discussion

*Preparation of ( $\beta$ ) $6\text{SbF}_3 \cdot 5\text{SbF}_5$ .*—Crystalline ( $\beta$ ) $6\text{SbF}_3 \cdot 5\text{SbF}_5$  was prepared by the reaction of  $\text{SbF}_3 \cdot \text{SbF}_5$  and a slight

excess of phosphorous trifluoride, relative to equation (1) of Table 1, in liquid arsenic trifluoride. The Raman spectrum of the bulk material was attributable to ( $\beta$ ) $6\text{SbF}_3 \cdot 5\text{SbF}_5$ , but it is possible that other species were present which were not detected by Raman spectroscopy. Several individual crystals were identified as ( $\beta$ ) $6\text{SbF}_3 \cdot 5\text{SbF}_5$  by Raman spectroscopy and X-ray precession photography. The weight of product corresponded to the formation of  $\text{SbF}_{3.25}$  rather than the expected  $\text{SbF}_{3.91}$ . This may be accounted for by the presence of small amounts of arsenic trifluoride, antimony pentafluoride, or  $\text{SbF}_5$  rich species (e.g.  $\text{SbF}_3 \cdot 2\text{SbF}_5 \cdot 2\text{AsF}_3$ )<sup>16</sup> in the  $\text{SbF}_3 \cdot \text{SbF}_5$  starting materials, or loss through solubility of the product in  $\text{AsF}_3$ . Similar low product weights were found for analogous reactions of  $\text{SbF}_3 \cdot \text{SbF}_5$  with a large excess of phosphorous trifluoride leading to  $3\text{SbF}_3 \cdot \text{SbF}_5$ ,<sup>5</sup> ( $\beta$ ) $6\text{SbF}_3 \cdot 5\text{SbF}_5$  was also prepared by the reaction of antimony pentafluoride and phosphorous trifluoride according to equation (2), Table 1; the product was a mixture. ( $\beta$ ) $6\text{SbF}_3 \cdot 5\text{SbF}_5$  and  $5\text{SbF}_3 \cdot 3\text{SbF}_5$  were unambiguously identified in both reactions (2i) and (2ii) (Table 1), and in addition, crystals with a cubic unit cell,  $a = 10.1(1)$  Å (possibly  $\text{H}_3\text{O}^+ \text{SbF}_6^-$ ),<sup>10</sup> were identified in one of the reactions [(2i), Table 1]. The course of a similar reaction carried out in sulphur dioxide rather than arsenic trifluoride solution [(2iii), Table 1] was different, and during the reaction a blue paste was formed. A similar blue colour was observed in the products of the reaction of antimony metal and antimony pentafluoride in sulphur dioxide solution.

The preferred route to ( $\beta$ ) $6\text{SbF}_3 \cdot 5\text{SbF}_5$  is by the reaction of iodine and a slight excess of antimony pentafluoride relative to equation (3) (Table 1), in sulphur dioxide solution. The product appeared to be homogeneous and the Raman spectrum of the bulk material was identical to that of single crystals. All the crystals that were examined by Raman spectroscopy and X-ray precession photography were shown unambiguously to be ( $\beta$ ) $6\text{SbF}_3 \cdot 5\text{SbF}_5$ . When a very large excess of antimony pentafluoride was used [reaction (3iii), Table 1] a mixture of  $\text{SbF}_3 \cdot \text{SbF}_5$ <sup>2</sup> and ( $\beta$ ) $6\text{SbF}_3 \cdot 5\text{SbF}_5$  was produced. The weights of reduced products were rather low, and those of  $\text{I}_2\text{Sb}_2\text{F}_{11}$  rather high. It is possible that some of the more finely divided antimony fluoride product passed through the coarse sintered glass frit during the numerous washings and filtrations of the product, or that the product has some solubility in  $\text{SO}_2$ . The high weight of  $\text{I}_2\text{Sb}_2\text{F}_{11}$  may also reflect some incorporation of solvent and/or  $\text{I}_2\text{Sb}_3\text{F}_{16}$  with the product. Satisfactory weights and elemental analyses were obtained for  $\text{I}_2\text{Sb}_2\text{F}_{11}$  prepared similarly,<sup>9</sup> but in arsenic trifluoride solution only after the product had been heated at  $100^\circ\text{C}$  and subjected to a dynamic vacuum overnight. In this work the products were routinely subjected to a dynamic vacuum overnight at room temperature.

**Table 3.** Vibrational spectra (values in  $\text{cm}^{-1}$ ) of  $(\beta)6\text{SbF}_3 \cdot 5\text{SbF}_5$  and related compounds

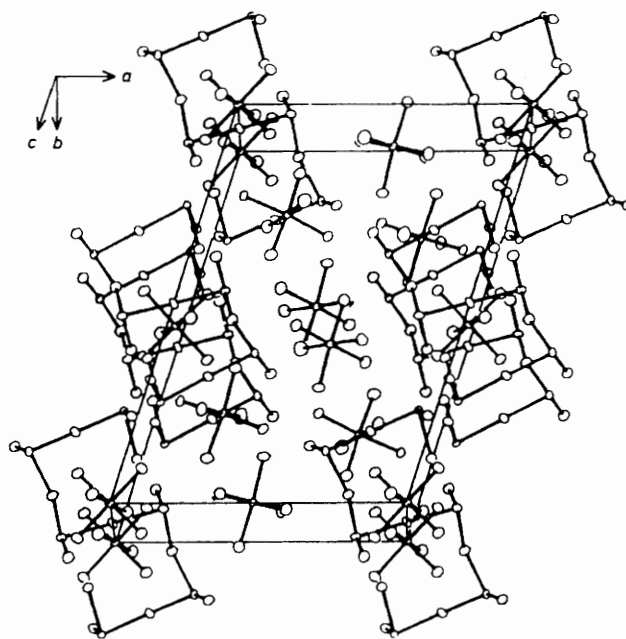
$\text{SbF}_3 \cdot \text{SbF}_5$ (A) <sup>a</sup> Raman	$\text{SbF}_3 \cdot \text{SbF}_5$ (B) <sup>a</sup> Raman	$(\alpha)6\text{SbF}_3 \cdot 5\text{SbF}_5$ <sup>b</sup> Raman	$(\beta)6\text{SbF}_3 \cdot 5\text{SbF}_5$ <sup>c</sup>			Tentative assignment for $(\beta)6\text{SbF}_3 \cdot 5\text{SbF}_5$ <sup>c</sup>
			Single crystal Raman	Bulk material Raman	Bulk material <sup>d</sup> I.r.	
719vw						} $\text{SbF}_6^-$ ( $\nu_1, \nu_3$ )
700m						
685m						
678m	678w,br		680 (0.9) <sup>f</sup>	681 (0.6)	680s	
668ms	658ms	663w,sh	659 (5.2)	659 (5.7)	670s	
642s	651s	654s	651 (10.0)	652 (10.0)	635s	
	625w,br		622 (0.4)	622 (0.4)	610s	} <sup>g</sup>
605ms	578m,br		578 (4.3)	577 (3.7)	570w	} $\text{Sb}_6\text{F}_{13}^{5+}$ (cation) and/or $\text{SbF}_6^-$ ( $\nu_2$ )
555mw	563m,sh,br	582m,br	564 (1.6)	566 (3.0)	535w	
495mw,br	~521m,vbr	490vw,br	519w,vbr			} Sb-F-Sb bridging stretch?
456m,vbr	~445m,vbr	445vw,br	447vbr (1.8)			
298m	295w,sh		294 (0.6)	294 (0.4)		} $\text{SbF}_6^-$ ( $\nu_3$ )
276mw	280mw	288m,br	282 (1.5)	282 (1.6)		
206w	~139w,br					Lattice vibrations

<sup>a</sup> Reported in ref. 1. <sup>b</sup> Reported in ref. 4. <sup>c</sup> This work; the relative intensities of the peaks are given in parentheses. <sup>d</sup> Powder between AgCl plates. Spectrum obtained in the region 450–4 000  $\text{cm}^{-1}$ . No peaks above 700  $\text{cm}^{-1}$  were observed. <sup>e</sup> Assignments made by comparison with those for  $\text{SbF}_6^-$  given in G. M. Begun and A. C. Rutenberg, *Inorg. Chem.*, 1967, 6, 2212. <sup>f</sup> Relative intensities of Raman spectra of single crystals obtained at different orientations were very similar, but were not absolutely identical. <sup>g</sup> Broad band with features at the indicated frequencies.

Interestingly, iodine, and a slight excess of antimony pentafluoride relative to that calculated according to equations (3) and (4) in Table 1, in arsenic trifluoride rather than sulphur dioxide solution, led to  $\text{SbF}_3 \cdot \text{SbF}_5$  and not  $(\beta)6\text{SbF}_3 \cdot 5\text{SbF}_5$ .<sup>9</sup> Our attempt to repeat the reported preparation of  $\text{SbF}_3 \cdot \text{SbF}_5$  (B) [ $(\beta)6\text{SbF}_3 \cdot 5\text{SbF}_5$ ], by the reaction of antimony metal and antimony pentafluoride in sulphur dioxide solution, gave the genuine 1:1 adduct  $\text{SbF}_3 \cdot \text{SbF}_5$ .<sup>2</sup> The nature of the product may reflect the magnitude of the excess [reaction (5), Table 1] of antimony pentafluoride (relative amounts were not given in the earlier work),<sup>2</sup> and the state of division of the antimony, the amount of sulphur dioxide, whether or not the mixture was mechanically stirred (ours were not), and a variety of other factors.

The  $(\alpha)6\text{SbF}_3 \cdot 5\text{SbF}_5$ <sup>3</sup> was prepared by the direct fluorination of elemental antimony, *i.e.* at high temperature, while  $(\beta)6\text{SbF}_3 \cdot 5\text{SbF}_5$  was prepared at room temperature in solution. Thus the  $\alpha$  phase is a high-temperature phase and the  $\beta$  material the low-temperature phase of  $6\text{SbF}_3 \cdot 5\text{SbF}_5$ .

**Vibrational Spectrum of  $(\beta)6\text{SbF}_3 \cdot 5\text{SbF}_5$ .**—The Raman spectra of single crystals and bulk  $(\beta)6\text{SbF}_3 \cdot 5\text{SbF}_5$  were identical to the reported spectra of  $\text{SbF}_3 \cdot \text{SbF}_5$  (B)<sup>1</sup> (see Table 3), and identical in every feature to a spectrum of an authentic sample of  $\text{SbF}_3 \cdot \text{SbF}_5$  (B) kindly sent to us by Dr. P. A. W. Dean. The similarity in the structures of  $(\alpha)6\text{SbF}_3 \cdot 5\text{SbF}_5$  and  $(\beta)6\text{SbF}_3 \cdot 5\text{SbF}_5$  is reflected in the similarity of the Raman spectra (Table 3). A major peak at 659  $\text{cm}^{-1}$  and a minor peak at 680  $\text{cm}^{-1}$  in the Raman spectrum of the  $\beta$  phase clearly differentiates it from the  $\alpha$  phase. These peaks may reflect the different structures of  $\text{Sb}_6\text{F}_{13}^{5+}$  cations or reflect different distortions of  $\text{SbF}_6^-$  from regular octahedral symmetry. The vibrational spectrum of  $(\beta)6\text{SbF}_3 \cdot 5\text{SbF}_5$  appears to be dominated by that of the  $\text{SbF}_6^-$  anion. The vibrational spectrum of  $\text{Sb}_6\text{F}_{13}^{5+}$  is either weak, or is masked by that of the anion. The Raman spectrum of  $3\text{SbF}_3 \cdot \text{SbF}_5$ , containing the polymeric  $(\text{Sb}_3\text{F}_8^+)_n$  cation and  $\text{SbF}_6^-$  anions, was also largely attributable to distorted  $\text{SbF}_6^-$  anions.<sup>5</sup>

**Figure 1.** Crystal packing of  $(\beta)6\text{SbF}_3 \cdot 5\text{SbF}_5$ 

**The X-Ray Crystal Structure of  $(\beta)6\text{SbF}_3 \cdot 5\text{SbF}_5$ .**—The crystal packing of  $(\beta)6\text{SbF}_3 \cdot 5\text{SbF}_5$  is shown in Figure 1. Atoms are connected which are separated by less than 2.16 Å. The bond distances and bond angles are given in Tables 4 and 5. The structure can be considered as made up of discrete  $\text{SbF}_6^-$  anions and  $\text{Sb}_6\text{F}_{13}^{5+}$  cations with considerable cation–anion interactions. The  $\text{Sb}_6\text{F}_{13}^{5+}$  cation can be identified (Figure 2) if fluorine contacts to the  $\text{Sb}^{\text{III}}$  atoms greater than 2.150 Å are not included. This cut-off point has been used by other workers<sup>2,3</sup> to define discrete antimony–fluorine units. Figure 3 shows the

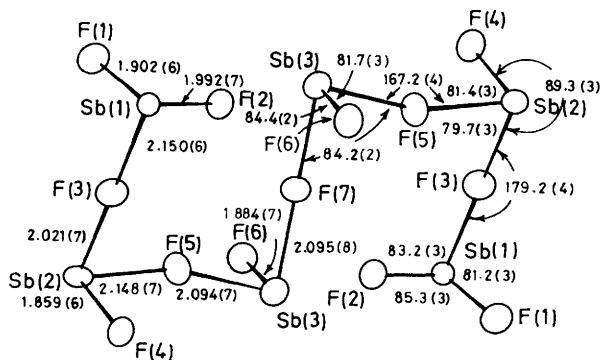


Figure 2.  $\text{Sb}_6\text{F}_{13}^{5+}$  cation in  $(\beta)\text{6SbF}_3 \cdot 5\text{SbF}_5$  with Sb-F distances ( $\text{\AA}$ )  $\leq 2.15 \text{\AA}$  and angles ( $^\circ$ )

$\text{Sb}_6\text{F}_{13}^{5+}$  cation with fluorine contacts up to  $3.55 \text{\AA}$ . The  $\text{Sb}_6\text{F}_{13}^{5+}$  cation consists of two different  $\text{SbF}_2^+$  and a central  $\text{Sb}_2\text{F}_5^+$  unit, when contacts greater than  $2.147 \text{\AA}$  are excluded. The central  $\text{Sb}_2\text{F}_5^+$  unit is made up of two  $\text{Sb}(3)\text{F}(5)\text{F}(6)$  units which are *trans* to each other, linearly bridged by  $\text{F}(7)$  which is on an inversion centre. The various geometries of  $\text{Sb}_2\text{F}_5^+$  cations have been discussed.<sup>5,6</sup> The  $\text{Sb}(1)\text{F}(1)\text{F}(2)$  and  $\text{Sb}(2)\text{F}(3)\text{F}(4)$  groups of atoms form the two  $\text{SbF}_2^+$  units.  $\text{SbF}_2^+$  units have been identified in  $(\alpha)\text{6SbF}_3 \cdot 5\text{SbF}_5$ ,<sup>3</sup> and said to be present in  $\text{M}^+\text{SbF}_2^+\text{SO}_4^{2-}$  ( $\text{M} = \text{Rb}$  or  $\text{Cs}$ )<sup>17</sup> and  $\text{K}^+\text{SbF}_2^+\text{HPO}_4^{2-}$ .<sup>18</sup> The cation  $\text{Sb}_6\text{F}_{13}^{5+}$  in  $(\beta)\text{6SbF}_3 \cdot 5\text{SbF}_5$  is twisted with a dihedral angle  $\text{Sb}(1)\text{Sb}(2)\text{Sb}(3)\text{Sb}(3)$  of  $29.3(3)^\circ$ .

Figure 4 was constructed on the basis of the data available for  $(\alpha)\text{6SbF}_3 \cdot 5\text{SbF}_5$ .<sup>3</sup> The shape of the  $\text{Sb}_6\text{F}_{13}^{5+}$  cation in  $(\beta)\text{6SbF}_3 \cdot 5\text{SbF}_5$  closely resembles that of  $(\alpha)\text{6SbF}_3 \cdot 5\text{SbF}_5$ . Both are made up of linearly fluorine-bridged  $\text{Sb}_2\text{F}_5^+$  cations of *trans* symmetry and two  $\text{SbF}_2^+$  units. Bond distances and angles within these units are similar. The  $\text{Sb}_6\text{F}_{13}^{5+}$  cations in  $(\alpha)\text{6SbF}_3 \cdot 5\text{SbF}_5$  are connected together by a distinctive double bridge with Sb-F distances  $2.01$  and  $2.31 \text{\AA}$  (Figure 4). The bridging interaction  $\text{Sb}(3)\text{F}(7)''$  of  $2.31 \text{\AA}$  is the strongest secondary contact to the  $\text{Sb}_6\text{F}_{13}^{5+}$  cation in  $(\alpha)\text{6SbF}_3 \cdot 5\text{SbF}_5$ .

In  $(\beta)\text{6SbF}_3 \cdot 5\text{SbF}_5$ , a bridging bond [ $\text{Sb}(1)\text{F}(51)$  at  $2.273(6) \text{\AA}$ ] of comparable strength to those in the cation is found between the anion and the cation. Figure 3 and Table 4 show that the  $\text{Sb}_6\text{F}_{13}^{5+}$  unit in  $(\beta)\text{6SbF}_3 \cdot 5\text{SbF}_5$  is relatively isolated from other  $\text{Sb}_6\text{F}_{13}^{5+}$  cations with nearest contacts to neighbouring  $\text{SbF}_6^-$  units. The cations in  $(\beta)\text{6SbF}_3 \cdot 5\text{SbF}_5$  are joined by the contacts  $\text{Sb}(1)\text{F}(6)'$  at  $2.682(8) \text{\AA}$  and  $\text{Sb}(1)\text{F}(1)'$  at  $2.965(6) \text{\AA}$  as shown in Figure 3. There are no other cation-anion contacts less than  $3.55 \text{\AA}$ .

The total bond valence, as defined by Brown,<sup>19,20</sup> of each Sb is 5 or 3 and each fluorine is 1 (Table 4). Thus the three bond valences of the  $\text{Sb}^{\text{III}}$  cations are distributed over the various strong and weak antimony-fluorine bonds, and the presence of oxygen (which can be mistaken for fluorine), can be ruled out.

*Co-ordination around antimony(III) atoms in the cation.* The primary co-ordination sphere around each antimony atom can be defined as that which contains all the fluorine atoms within  $2.15 \text{\AA}$ . The identification of secondary co-ordination spheres is not always very clear-cut. Co-ordination spheres are identified when there is a noticeable gap in the bond lengths (hence bond valences). The bond distances, bond valences, and the types of co-ordination spheres to which the fluorine atoms belong are listed in Table 4.

*Co-ordination around Sb(1).* The primary co-ordination unit around  $\text{Sb}(1)$  can be considered as consisting of  $\text{Sb}(1)\text{F}(1)\text{F}(2)\text{F}(3)$ , all of which belong to the  $\text{Sb}_6\text{F}_{13}^{5+}$  cation (Figure 2).

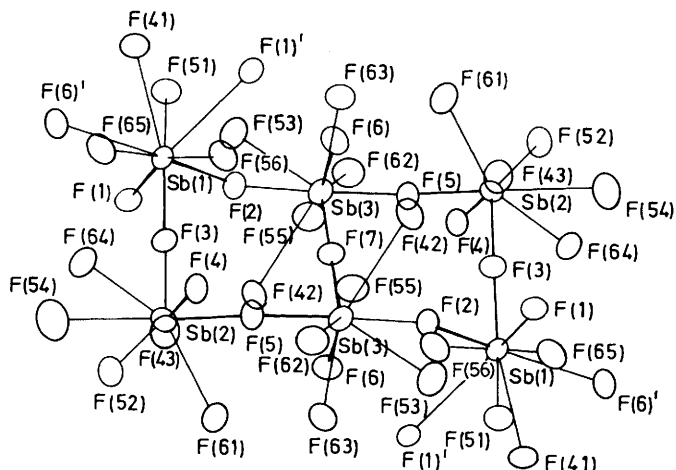


Figure 3.  $\text{Sb}_6\text{F}_{13}^{5+}$  cation in  $(\beta)\text{6SbF}_3 \cdot 5\text{SbF}_5$  including the contacts  $\leq 3.55 \text{\AA}$ . All the fluorine atoms with double digits have their primary contacts to the anions. All the fluorine atoms with a single digit have their primary contacts to the  $\text{Sb}_6\text{F}_{13}^{5+}$  cation.  $\text{F}(1)'$  and  $\text{F}(6)'$  have their primary contacts to other  $\text{Sb}_6\text{F}_{13}^{5+}$  units

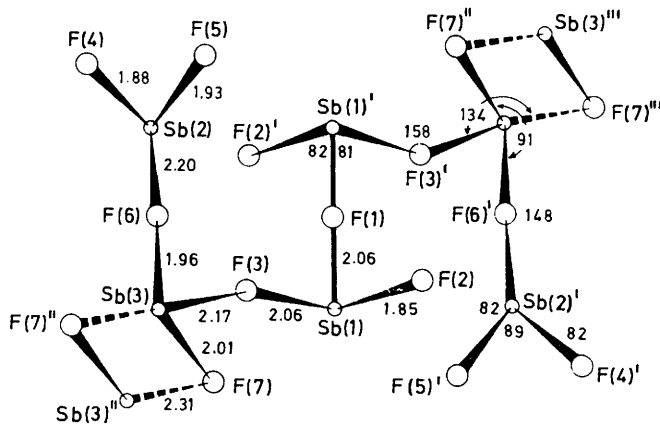


Figure 4. Illustration of the  $\text{Sb}_6\text{F}_{13}^{5+}$  cation including the intercation double bridge [ $\text{Sb}(3)\text{F}(7)$ ,  $\text{Sb}(3)'\text{F}(7)'$ ] in  $(\alpha)\text{6SbF}_3 \cdot 5\text{SbF}_5$ , reported by Edwards and Slim<sup>3</sup>

In terms of valence shell electron pair repulsion (v.s.e.p.r.) theory,<sup>21</sup> this is expressed as  $\text{AX}_3\text{E}$  where three fluorine atoms and the lone pair occupy the vertices of a tetrahedron. The values of the two angles  $\text{F}(2)\text{Sb}(1)\text{F}(3)$  at  $83.2(3)^\circ$  and  $\text{F}(1)\text{Sb}(1)\text{F}(3)$  at  $81.2(3)^\circ$  do not conform with the v.s.e.p.r. model requirement that  $\text{F}(1)\text{Sb}(1)\text{F}(3) > \text{F}(2)\text{Sb}(1)\text{F}(3)$ , as  $\text{Sb}(1)\text{F}(1)$  is shorter than  $\text{Sb}(1)\text{F}(2)$ . Although the exact reasons for this inconsistency are not clear, it is possible that the strong bridging interactions between  $\text{F}(2)$  and  $\text{Sb}(3)$  and  $\text{F}(3)$  and  $\text{Sb}(2)$  may be factors.

Inclusion of the cation-anion bridge  $\text{Sb}(1)\text{F}(51)$  at  $2.273(6) \text{\AA}$  to this primary co-ordination unit gives rise to a new unit,  $\text{Sb}(1)\text{F}(1)\text{F}(2)\text{F}(3)\text{F}(51)$  which can be described as having  $\text{AX}_4\text{E}$  trigonal-bipyramidal geometry as shown in Figure 5(a). The axial positions are taken by  $\text{F}(3)$  and  $\text{F}(51)$  while the equatorial positions of the trigonal bipyramid are taken by  $\text{F}(1)$ ,  $\text{F}(2)$ , and the lone pair. The co-ordination sphere around  $\text{Sb}(1)$  is completed by the inclusion of five more long contacts of which four,  $\text{F}(1)'$ ,  $\text{F}(6)'$ ,  $\text{F}(56)$ , and  $\text{F}(65)$ , are capping the faces of the trigonal bipyramid around the lone pair and the last one,  $\text{F}(41)$ , is bridging an edge. A similar description of long contacts to

**Table 4.** Bond distances, corresponding bond valences<sup>a</sup> and their correlation to structure types in (β)6SbF<sub>3</sub>·5SbF<sub>5</sub>

Sb <sup>III</sup> (1)		F(1)	F(2)	F(3)	F(51) <sup>b</sup>	F(56) <sup>b</sup>	F(6)'	F(41) <sup>b</sup>	F(65) <sup>b</sup>	F(1)'	Total bond valence
	Bond valence	0.77	0.65	0.49	0.40	0.22	0.22	0.19	0.15	0.15	
	Bond length	1.902(6)	1.992(7)	2.150(6)	2.273(6)	2.678(7)	2.682(8)	2.795(7)	2.949(8)	2.965(6)	
Structural type <sup>d</sup>		AX <sub>3</sub> E									
		AX <sub>4</sub> E									
		AXY <sub>4</sub> E									
		AX <sub>4</sub> Y <sub>4</sub> Y'E or AXY <sub>4</sub> Z <sub>4</sub> E									
Sb <sup>III</sup> (2)		F(4)	F(3)	F(5)	F(64) <sup>b</sup>	F(61) <sup>b</sup>	F(52) <sup>b</sup>	F(43) <sup>b</sup>	F(54) <sup>b</sup>		3.03 <sup>e</sup>
	Bond valence	0.84	0.61	0.49	0.27	0.25	0.24	0.19	0.14		
	Bond length	1.859(6)	2.021(7)	2.148(7)	2.518(7)	2.589(8)	2.612(7)	2.772(7)	2.994(8)		
Structural type <sup>d</sup>		AX <sub>3</sub> E									
		AX <sub>4</sub> E									
		AXY <sub>3</sub> E									
		AX <sub>3</sub> Y <sub>3</sub> Y' <sub>2</sub> E or AX <sub>4</sub> Y <sub>4</sub> E									
Sb <sup>III</sup> (3)		F(6)	F(5)	F(7)	F(2)	F(63) <sup>b</sup>	F(42) <sup>b</sup>	F(53) <sup>b</sup>	F(62) <sup>b</sup>	F(55) <sup>b</sup>	3.04 <sup>f</sup>
	Bond valence	0.80	0.54	0.54	0.37	0.26	0.16	0.15	0.12	0.11	
	Bond length	1.884(7)	2.094(7)	2.095(8)	2.311(7)	2.545(7)	2.932(8)	2.974(8)	3.146(7)	3.258(7)	
Structural type <sup>d</sup>		AX <sub>3</sub> E									
		AX <sub>4</sub> E									
		AXY <sub>4</sub> E									
		AX <sub>4</sub> Y <sub>4</sub> Y'E or AXY <sub>4</sub> Z <sub>2</sub> Z' <sub>2</sub> E									

Bond distances and the corresponding bond valences in the SbF<sub>6</sub><sup>-</sup> anions

Sb <sup>V</sup> (4)		F(41)	F(41)'	F(42)	F(42)'	F(43)	F(43)'	4.92
	Bond valence	0.86	0.86	0.78	0.78	0.82	0.82	
	Bond length	1.869(7)	1.869(7)	1.893(7)	1.893(7)	1.880(7)	1.880(7)	
Sb <sup>V</sup> (5)		F(51)	F(52)	F(53)	F(54)	F(55)	F(56)	5.18
	Bond valence	0.69	0.84	0.87	0.96	0.91	0.91	
	Bond length	1.927(6)	1.875(7)	1.864(8)	1.839(8)	1.855(8)	1.853(7)	
Sb <sup>V</sup> (6)		F(61)	F(62)	F(63)	F(64)	F(65)	F(66)	5.12
	Bond valence	0.86	0.92	0.72	0.76	0.90	0.96	
	Bond length	1.868(8)	1.850(7)	1.916(7)	1.901(7)	1.856(7)	1.840(8)	

<sup>a</sup> All bond valences less than 0.08 are omitted. <sup>b</sup> Anionic fluorine atom bridged to a cationic antimony atom. <sup>c</sup> Contribution from anions 0.96. <sup>d</sup> Designation of geometry follows that of Gillespie.<sup>21,22</sup> <sup>e</sup> Contribution from anions 0.95. <sup>f</sup> Contribution from anions 0.80.

**Table 5.** Bond angles (°) with estimated deviations in parentheses**(a) Involving Sb-F ≤ 2.5 Å**

F(1)-Sb(1)-F(2)	85.3(3)	F(41)-Sb(4)-F(43)	90.8(3)	F(54)-Sb(5)-F(55)	90.1(4)
F(1)-Sb(1)-F(3)	81.2(3)	F(41')-Sb(4)-F(43)	89.2(3)	F(54)-Sb(5)-F(56)	175.6(4)
F(1)-Sb(1)-F(51)	81.5(3)	F(42)-Sb(4)-F(42')	180.0	F(55)-Sb(5)-F(56)	88.8(4)
F(2)-Sb(1)-F(3)	83.2(3)	F(42)-Sb(4)-F(43)	90.2(3)	F(61)-Sb(6)-F(62)	90.3(3)
F(2)-Sb(1)-F(51)	84.2(2)	F(42)-Sb(4)-F(43')	89.8(3)	F(61)-Sb(6)-F(63)	86.1(3)
F(3)-Sb(1)-F(51)	159.3(2)	F(43)-Sb(4)-F(43')	180.0	F(61)-Sb(6)-F(64)	174.3(3)
F(3)-Sb(2)-F(4)	89.3(3)	F(51)-Sb(5)-F(52)	175.7(3)	F(61)-Sb(6)-F(65)	89.9(3)
F(3)-Sb(2)-F(5)	79.7(3)	F(51)-Sb(5)-F(53)	86.6(3)	F(61)-Sb(6)-F(66)	93.8(4)
F(4)-Sb(2)-F(5)	81.4(3)	F(51)-Sb(5)-F(54)	88.9(3)	F(62)-Sb(6)-F(63)	90.4(3)
F(2)-Sb(3)-F(5)	153.8(3)	F(51)-Sb(5)-F(55)	89.3(3)	F(62)-Sb(6)-F(64)	90.2(3)
F(2)-Sb(3)-F(6)	76.9(3)	F(51)-Sb(5)-F(56)	86.8(3)	F(62)-Sb(6)-F(65)	175.9(3)
F(2)-Sb(3)-F(7)	79.0(2)	F(52)-Sb(5)-F(53)	89.6(3)	F(62)-Sb(6)-F(66)	92.3(4)
F(5)-Sb(3)-F(6)	81.7(3)	F(52)-Sb(5)-F(54)	93.0(3)	F(63)-Sb(6)-F(64)	88.1(3)
F(5)-Sb(3)-F(7)	84.2(2)	F(52)-Sb(5)-F(55)	94.5(3)	F(63)-Sb(6)-F(65)	85.5(3)
F(6)-Sb(3)-F(7)	84.4(2)	F(52)-Sb(5)-F(56)	91.3(3)	F(63)-Sb(6)-F(66)	177.4(4)
F(41)-Sb(4)-F(41')	180.0	F(53)-Sb(5)-F(54)	90.4(4)	F(64)-Sb(6)-F(65)	89.2(3)
F(41)-Sb(4)-F(42)	90.7(3)	F(53)-Sb(5)-F(55)	175.8(4)	F(64)-Sb(6)-F(66)	91.9(4)
F(41')-Sb(4)-F(42)	89.3(3)	F(53)-Sb(5)-F(56)	90.4(4)	F(65)-Sb(6)-F(66)	91.8(4)

**(b) Involving 2.5 ≤ Sb-F ≤ 3.55 Å**

F(1)-Sb(1)-F(1')	141.9(2)	F(5)-Sb(2)-F(64)	144.0(3)	F(2)-Sb(3)-F(42)	67.8(2)
F(1)-Sb(1)-F(6')	69.7(2)	F(43)-Sb(2)-F(52)	133.5(2)	F(2)-Sb(3)-F(53)	65.4(2)
F(1)-Sb(1)-F(41)	127.4(2)	F(43)-Sb(2)-F(54)	63.2(2)	F(2)-Sb(3)-F(62)	129.0(2)
F(1)-Sb(1)-F(56)	148.1(2)	F(43)-Sb(2)-F(61)	101.2(2)	F(2)-Sb(3)-F(63)	107.0(2)
F(1)-Sb(1)-F(65)	116.1(3)	F(43)-Sb(2)-F(64)	116.8(2)	F(5)-Sb(3)-F(42)	122.2(2)
F(1')-Sb(1)-F(2)	70.9(2)	F(52)-Sb(2)-F(54)	83.7(2)	F(5)-Sb(3)-F(53)	134.9(3)
F(1')-Sb(1)-F(3)	123.1(2)	F(52)-Sb(2)-F(61)	66.6(2)	F(5)-Sb(3)-F(62)	76.0(2)
F(1')-Sb(1)-F(6')	119.2(2)	F(3)-Sb(2)-F(43)	70.9(2)	F(5)-Sb(3)-F(63)	79.8(3)
F(1')-Sb(1)-F(41)	59.3(2)	F(3)-Sb(2)-F(52)	137.0(2)	F(6)-Sb(3)-F(42)	136.2(3)
F(1')-Sb(1)-F(51)	67.3(2)	F(3)-Sb(2)-F(54)	79.8(2)	F(6)-Sb(3)-F(53)	102.3(3)
F(1')-Sb(1)-F(56)	60.4(2)	F(3)-Sb(2)-F(61)	153.9(3)	F(6)-Sb(3)-F(62)	125.2(3)
F(1')-Sb(1)-F(65)	100.3(2)	F(3)-Sb(2)-F(64)	72.4(3)	F(6)-Sb(3)-F(63)	71.9(3)
F(2)-Sb(1)-F(6')	149.4(2)	F(4)-Sb(2)-F(43)	149.8(3)	F(7)-Sb(3)-F(42)	64.8(2)
F(2)-Sb(1)-F(41)	128.7(2)	F(4)-Sb(2)-F(52)	76.4(3)	F(7)-Sb(3)-F(53)	140.7(2)
F(2)-Sb(1)-F(56)	84.7(3)	F(4)-Sb(2)-F(54)	137.0(3)	F(7)-Sb(3)-F(62)	140.3(1)
F(2)-Sb(1)-F(65)	142.7(2)	F(4)-Sb(2)-F(61)	86.5(3)	F(7)-Sb(3)-F(63)	153.0(2)
F(3)-Sb(1)-F(6')	108.9(2)	F(4)-Sb(2)-F(64)	76.1(3)	F(42)-Sb(3)-F(53)	85.9(2)
F(3)-Sb(1)-F(41)	133.7(2)	F(5)-Sb(2)-F(43)	72.9(3)	F(42)-Sb(3)-F(62)	97.5(2)
F(3)-Sb(1)-F(56)	67.7(2)	F(5)-Sb(2)-F(52)	135.7(2)	F(42)-Sb(3)-F(63)	142.2(2)
F(3)-Sb(1)-F(65)	71.5(2)	F(5)-Sb(2)-F(54)	135.6(3)	F(53)-Sb(3)-F(62)	65.1(2)
F(6)-Sb(1)-F(41)	62.5(2)	F(5)-Sb(2)-F(61)	74.2(3)	F(53)-Sb(3)-F(63)	59.9(2)
F(6)-Sb(1)-F(51)	75.2(2)	F(52)-Sb(2)-F(64)	64.8(2)	F(62)-Sb(3)-F(63)	55.3(2)
F(6)-Sb(1)-F(56)	125.8(2)	F(54)-Sb(2)-F(61)	119.8(2)		
F(6)-Sb(1)-F(65)	67.0(2)	F(54)-Sb(2)-F(64)	61.0(2)		
F(41)-Sb(1)-F(51)	66.6(2)	F(61)-Sb(2)-F(64)	130.9(3)		
F(41)-Sb(1)-F(56)	81.6(2)				
F(41)-Sb(1)-F(65)	63.4(2)				
F(51)-Sb(1)-F(56)	127.3(2)				
F(51)-Sb(1)-F(65)	126.9(2)				
F(56)-Sb(1)-F(65)	60.8(2)				

Sb<sup>III</sup> species has been given by Gillespie and Sawyer.<sup>22</sup> In v.s.e.p.r. terms the overall geometry shown in Figure 5(a) can be expressed as AX<sub>4</sub>Y<sub>4</sub>Y'E where face-capping contacts are designated Y<sub>4</sub> and the edge-bridging contact designated Y'. However, F(6) and F(65) are markedly shifted from their ideal positions to positions between the face-capping and edge-bridging positions. The AX<sub>4</sub>Y<sub>4</sub>Y'E type of geometry has been observed in other compounds, e.g. KSb<sub>2</sub>F<sub>7</sub>·3KNO<sub>3</sub>.<sup>22,23</sup> Alternatively, the geometry can be expressed in v.s.e.p.r. terms as AX<sub>4</sub>Y<sub>4</sub>Z<sub>4</sub>E where the shortest bond, Sb(1)-F(1), is opposite to the lone pair, as illustrated in Figure 5(b). The remaining fluorine atoms, F(2), F(3), F(6'), and F(51), designated Y<sub>4</sub>, are in a plane perpendicular to Sb(1)-F(1), completing the AX<sub>4</sub>Y<sub>4</sub>E octahedral geometry. F(1'), F(41), F(56), and F(65), designated Z<sub>4</sub>, cap the four faces of the octahedron around the lone pair. A deficiency in this model is the essential equality of the bond

lengths of the primary contact (Y) [Sb(1)-F(6') 2.682(8) Å] and the secondary contact (Z) [Sb(1)-F(56) 2.678(7) Å]. The AX<sub>4</sub>Y<sub>4</sub>Z<sub>4</sub>E type geometry is found in other compounds, e.g. XeF<sub>5</sub><sup>+</sup>RuF<sub>6</sub><sup>-</sup>.<sup>22,24</sup> An examination of a model of Sb(1) and its interacting fluorine atoms led us to conclude that the geometry is closer to AX<sub>4</sub>Y<sub>4</sub>Y'E than AX<sub>4</sub>Y<sub>4</sub>Z<sub>4</sub>E.

*Co-ordination around Sb(2).* The primary co-ordination around Sb(2) within the cation contains F(3), F(4), and F(5) with an AX<sub>3</sub>E tetrahedral type of geometry (Figure 2). The overall geometry around Sb(2) can be expressed in v.s.e.p.r. terms as AX<sub>3</sub>Y<sub>3</sub>Y'<sub>2</sub>E. The secondary contacts F(43), F(61), and F(64), designated Y<sub>3</sub>, cap the faces of the tetrahedron around the lone pair. Two remaining long contacts to F(54) and F(52), designated Y<sub>2</sub>, bridge two edges as illustrated in Figure 6(a). However, the edge-bridging atom F(52) is slightly shifted towards the face-capping position. AX<sub>3</sub>Y<sub>3</sub>Y'<sub>2</sub>E type of co-

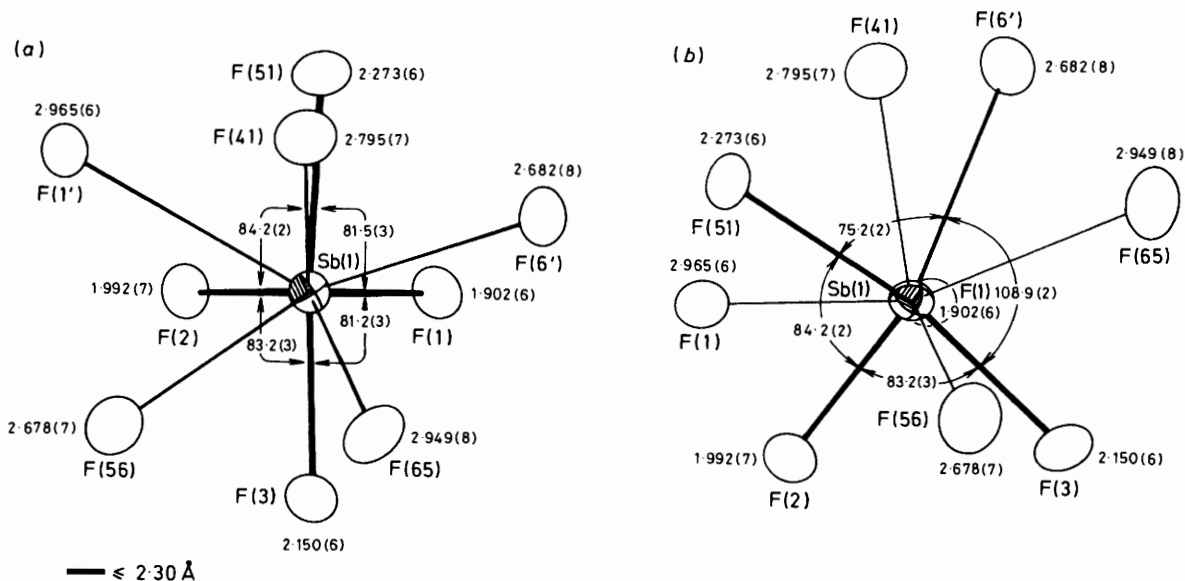


**Figure 5.** (a) Co-ordination around Sb(1) (including all Sb–F contacts  $\leq 3.55$  Å), illustrating an  $AX_4Y_4Y'E$  geometry where  $X_4 = F(1), F(2), F(3)$ , and  $F(51)$ ;  $Y_4 = F(1'), F(6'), F(65)$ , and  $F(56)$ ;  $Y' = F(41)$ ;  $F(1)Sb(1)F(2)$   $85.3(3)^\circ$ ,  $F(3)Sb(1)F(51)$   $159.3(2)^\circ$ ; (b) co-ordination around Sb(1) (including all Sb–F contacts  $\leq 3.55$  Å), illustrating an  $AX_4Z_4E$  geometry where  $X = F(1)$ ;  $Y_4 = F(2), F(3), F(51)$ , and  $F(6)$ ;  $Z_4 = F(56), F(65), F(41)$ , and  $F(1')$ ;  $F(1)Sb(1)F(2)$   $85.3(2)^\circ$ ,  $-F(3)$   $81.2(3)^\circ$ ,  $-F(6)$   $69.7(2)^\circ$ ,  $-F(51)$   $81.5(3)^\circ$

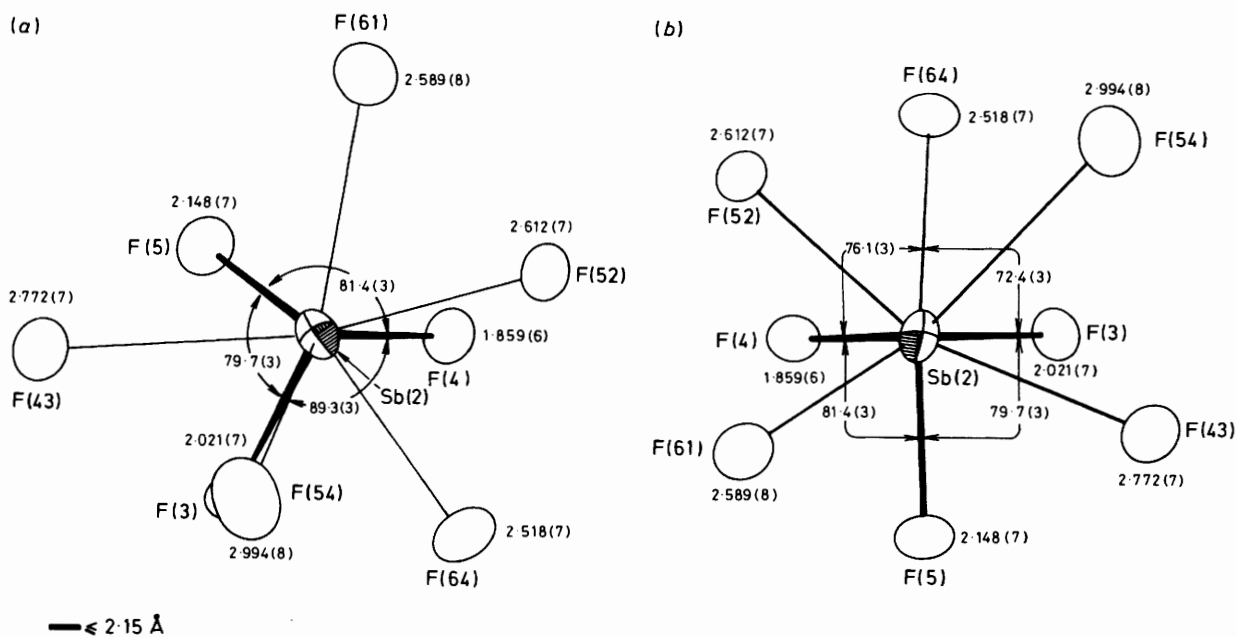


**Figure 6.** (a) Co-ordination around Sb(2) (including all Sb–F contacts  $\leq 3.55$  Å), illustrating an  $AX_3Y_3Y'E$  geometry where  $X_3 = F(3), F(4)$ , and  $F(5)$ ;  $Y_3 = F(43), F(61)$ , and  $F(64)$ ;  $Y'_2 = F(52)$  and  $F(54)$ ; (b) co-ordination around Sb(2) (including all contacts  $\leq 3.55$  Å), illustrating an  $AX_4Y_4E$  geometry where  $X_4 = F(3), F(4), F(5)$ , and  $F(64)$ ;  $Y_4 = F(43), F(61), F(52)$ , and  $F(54)$ ;  $F(3)Sb(2)F(4)$   $89.3(3)^\circ$ ,  $F(5)Sb(2)F(64)$   $144.0(3)^\circ$

ordination is found in other compounds, e.g.  $SbF_3 \cdot SbF_5$ ,<sup>2</sup>  $KSb_2F_7$ ,<sup>25</sup> and  $NaSb_3F_{10}$ .<sup>26</sup> Alternatively, the geometry can be expressed in v.s.e.p.r. terms as  $AX_4Y_4E$  where the two fluorine atoms  $F(3)$  and  $F(4)$  and the lone pair occupy the equatorial positions of the trigonal bipyramid  $AX_4E$ , while the axial positions are occupied by  $F(5)$  and  $F(64)$ . The four fluorine atoms  $F(52)$ ,  $F(61)$ ,  $F(54)$ , and  $F(43)$ , designated  $Y_4$ , cap the faces of the trigonal bipyramid around the lone pair as illustrated by Figure 6(b). It is interesting to note that the

fluorine atoms  $F(3)$ ,  $F(5)$ ,  $F(61)$ ,  $F(52)$ , and  $F(64)$ , which can be designated  $Y_5$ , lie in a pseudo-plane perpendicular to the  $Sb(2)F(4)$  bond. When  $F(4)$  is designated  $X$ , the geometry around  $Sb(2)$  can be expressed as (pseudo)  $AXY_5E$  type. However, the fluorine atoms in  $Y_5$  deviate markedly from planarity and hence the  $AXY_5E$  description of the structure is not appropriate.

The axial bond  $Sb(2)F(64)$  [ $2.518(7)$  Å] of the  $AX_4E$  trigonal bipyramid is relatively long compared to the other axial

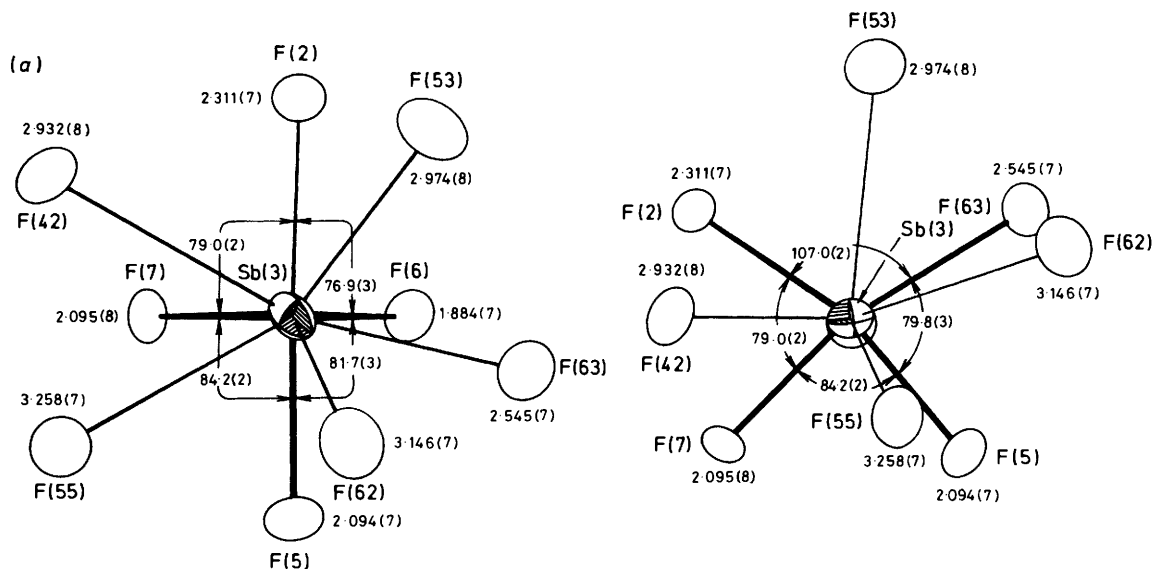


**Figure 7.** (a) Co-ordination around Sb(3) (including all contacts  $\leq 3.55$  Å), illustrating an  $AX_4Y_4Y'E$  geometry where  $X_4 = F(5), F(6), F(2),$  and  $F(7)$ ;  $Y_4 = F(42), F(53), F(62),$  and  $F(55)$ ;  $Y' = F(63)$ ;  $F(6)Sb(3)F(7)$  84.4(2),  $F(2)Sb(3)F(5)$  153.8(3)°; (b) co-ordination around Sb(3) (including all Sb–F contacts  $\leq 3.55$  Å), illustrating an  $AX_4Z_2Z'E$  geometry where  $X = F(6)$ ;  $Y_4 = F(5), F(7), F(2),$  and  $F(63)$ ;  $Z_2 = F(42)$  and  $F(53)$ ;  $Z'_2 = F(55)$  and  $F(62)$ ;  $Sb(3)F(6)$  1.884(7) Å;  $F(6)Sb(3)F(5)$  81.7(3),  $-F(7)$  84.4(2),  $-F(2)$  76.9(3),  $-F(63)$  71.9(3)°

bond  $Sb(2)F(5)$  [2.148(7) Å]. This illustrates the highly distorted nature of the  $AX_4E$  trigonal bipyramid. The structural designation of the fluorine atoms about Sb(2) is nearer  $AX_3Y_3Y_2E$  than  $AX_4Y_4E$ .

**Co-ordination around Sb(3).** The primary co-ordination around Sb(3) within the  $Sb_6F_{13}^{5+}$  cation is  $AX_3E$ , containing  $Sb(3)F(5)F(6)F(7)$  (Figure 2). According to the v.s.e.p.r. model the angle  $F(7)Sb(3)F(5)$  should be the smallest of the three angles around Sb(3) in this  $Sb(3)F(5)F(6)F(7)$  unit. However, the angle  $F(7)Sb(3)F(5)$  is slightly larger than  $F(5)Sb(3)F(6)$ . The  $F(6)Sb(3)F(7)$  angle may be affected by the formation of strong interactions of F(6) and F(7) with Sb(3) and Sb(2) respectively. The inclusion of  $Sb(3)F(2)$  at 2.311(7) Å makes the geometry around Sb(3) of the  $AX_4E$  trigonal-bipyramidal type where F(2), F(5), F(6), and F(7) are designated  $X_4$ . The geometry is illustrated in Figure 7(a). The co-ordination around Sb(3) is completed by the inclusion of five more contacts to F(42), F(55), F(62), and F(63) all of which are around the lone pair, Figure 7(a). This overall geometry can be described in v.s.e.p.r. terms as  $AX_4Y_4Y'E$  where four long contacts, F(55), F(42), F(53), and F(62), designated  $Y_4$ , cap the faces of the distorted trigonal bipyramid  $AX_4E$  around the lone pair. F(63) is located between the edge-bridging and face-capping positions of the trigonal bipyramid. The imperfect location (away from the edge-bridging position) of F(63) has apparently shifted F(62) and F(55) slightly away from their face-capping positions. Alternatively, the overall geometry can be described in v.s.e.p.r. terms as  $AXY_4Z_2Z'E$  where the shortest bond,  $Sb(3)F(6)$ , designated X, is opposite the lone pair. F(2), F(5), F(7), and F(63) designated  $Y_4$  are in a plane perpendicular to the lone-pair F(6) axis, to complete the  $AXY_4$  octahedral geometry around the Sb(3) as illustrated in Figure 7(b). The two long contacts around the lone pair, F(42) and F(53), designated  $Z_2$ , cap two faces of the octahedron. The other two long contacts, F(55) and F(62), which can be considered as edge-bridging contacts, have shifted slightly toward the face-capping positions. An examination of a model of the co-ordination around Sb(3) led us to conclude that the structure type around Sb(3) is nearer  $AX_4Y_4Y'E$  than  $AXY_4Z_2Z'E$ .

The  $Sb(4)F_6^-$  cation has a nearly perfect octahedral

geometry with a mean Sb–F distance of 1.881(7) Å. The  $Sb(5)F_6^-$  and  $Sb(6)F_6^-$  cations are slightly distorted octahedra with mean Sb–F distances of 1.869(7) and 1.840(8) Å respectively.

The structure is approximately close-packed with a volume per fluorine atom of 19.5 Å<sup>3</sup>. If it is assumed that the lone pair on the antimony atom occupies a volume equivalent to a fluorine atom, then the volume per fluorine atom becomes 17.1 Å<sup>3</sup> which is comparable to that of  $SbF_3$  (16.8 Å<sup>3</sup>).

### Acknowledgements

We thank the Natural Sciences and Engineering Research Council (Canada) for financial support and Drs. A. J. Edwards and J. H. Holloway for providing unpublished results and for helpful discussions and suggestions.

### References

- 1 T. Birchall, P. A. W. Dean, B. Della Valle, and R. J. Gillespie, *Can. J. Chem.*, 1973, **51**, 667.
- 2 R. J. Gillespie, D. R. Slim, and J. E. Vekris, *J. Chem. Soc., Dalton Trans.*, 1977, 971.
- 3 A. J. Edwards and D. R. Slim, *J. Chem. Soc., Chem. Commun.*, 1974, 178.
- 4 A. J. Hewitt, J. H. Holloway, and B. Frlc, *J. Fluorine Chem.*, 1980, **15**, 435.
- 5 W. A. S. Nandana, J. Passmore, D. C. N. Swindells, P. Taylor, P. S. White, and J. E. Vekris, *J. Chem. Soc., Dalton Trans.*, 1983, 619 and refs. therein.
- 6 W. A. S. Nandana, J. Passmore, P. S. White, and C-M. Wong, unpublished work.
- 7 A. J. Edwards, personal communication.
- 8 A. J. Edwards and J. H. Holloway, personal communication.
- 9 J. Passmore, W. A. S. Nandana, E. K. Richardson, and P. Taylor, *J. Fluorine Chem.*, 1980, **15**, 435 and refs. therein.
- 10 W. A. S. Nandana, J. Passmore, and P. S. White, unpublished work.
- 11 K. O. Christe, P. Charpin, E. Soulie, R. Bougon, J. Fawcett, and D. R. Russel, unpublished work.
- 12 W. W. Wilson, R. C. Thompson, and F. Aubke, *Inorg. Chem.*, 1980, **19**, 1489.

- 13 P. Main, 'MULTAN-80, A System of Computer Programs for the Automatic Solution of Crystal Structures from X-Ray Diffraction Data,' University of York, 1980.
- 14 'International Tables for X-Ray Crystallography,' Kynoch Press, Birmingham, 1974, vol. 4.
- 15 A. C. Larson and E. J. Gabe, 'Minimum Computer System for Complete Structure Determination—Computing in Crystallography,' eds. H. Schenk, R. Oltof-Hazekamp, H. van Koningsveld, and G. C. Bassi, Delft University Press, The Netherlands, 1978, pp. 81—89.
- 16 A. J. Edwards and K. I. Kallow, 8th European Symposium on Fluorine Chemistry, Jerusalem, Israel, 21—26 August, 1983, Abstract I-38.
- 17 R. Fourcade, M. Bourgault, B. Bonnet, and B. Ducourant, *J. Solid State Chem.*, 1982, **43**, 81.
- 18 S. Hurter, R. Mattes, and R. Rühl, *J. Solid State Chem.*, 1983, **46**, 204.
- 19 I. D. Brown, *J. Solid State Chem.*, 1974, **11**, 214.
- 20 I. D. Brown, *Chem. Soc. Rev.*, 1978, **7**, 359 and refs. therein.
- 21 R. J. Gillespie, 'Molecular Geometry,' Van Nostrand Reinhold, London, 1972.
- 22 R. J. Gillespie and J. F. Sawyer in 'Progress in Inorganic Chemistry,' ed. S. Lippard, Wiley Interscience, 1985, vol. 34.
- 23 A. A. Udovenko, L. M. Volkova, R. L. Davidovich, and M. A. Simonov, *Koord. Khim.*, 1979, **5**, 133.
- 24 N. Bartlett, M. Gennis, D. D. Gibler, B. K. Morrel, and A. Zalkin, *Inorg. Chem.*, 1973, **12**, 1717.
- 25 S. H. Mastin and R. R. Ryan, *Inorg. Chem.*, 1971, **10**, 1757.
- 26 R. Fourcade, G. Mascherpa, and E. Philippot, *Acta Crystallogr., Sect. B*, 1975, **31**, 2322.

Received 24th July 1984; Paper 4/1291